Bayesian modeling of HFC production pipeline suggests growth in unreported CFC by-product and feedstock production

Stephen Bourguet

stephen.bourguet@georgetown.edu

Georgetown University

Megan Lickley

Georgetown University https://orcid.org/0000-0001-5810-8784

Article

Keywords:

Posted Date: July 24th, 2024

DOI: https://doi.org/10.21203/rs.3.rs-4718479/v1

Additional Declarations: There is **NO** Competing Interest.

Bayesian modeling of HFC production pipeline suggests growth in unreported CFC by-product and feedstock production

Stephen Bourguet[1*] and Megan Lickley[1,2]

[1]Earth Commons, Georgetown University, Washington, DC 20057, USA
[2]Science, Technology, and International Affairs Program, Georgetown University, Washington, DC 20057, USA
[*]Corresponding author: stephen.bourguet@georgetown.edu

July 9, 2024

Abstract

Observationally-derived emissions of regulated ozone depleting substances (ODSs) must be scrutinized to maintain the progress made by the Montreal Protocol in protecting the stratospheric ozone layer. Recent observations of three chlorofluorocarbons (CFCs), CFC-113, CFC-114, and CFC-115, suggest that emissions of these compounds have been higher than expected given global reporting. These emissions have been associated with hydrofluorocarbon (HFC) production, which can require CFCs as feedstocks or generate CFCs as by-products, yet emissions from these pathways have not been rigorously quantified. Here, we develop a Bayesian framework to jointly infer emissions of CFC-113, CFC-114, CFC-115, and hydrochlorofluorocarbon HCFC-133a during HFC-134a and HFC-125 production. We estimate that feedstock usage in HFC-134a production accounted for 86% (75–92%) and 62% (46–74%) of CFC-113 and CFC-114 emissions, respectively, from 2015–2019, while by-product generation during HFC-125 production accounted for 81% (68–92%) of CFC-115 emissions. Our results suggest that unreported feedstock production in Article 5 countries may explain the unexpected atmospheric growth rates of CFC-113 and CFC-114, although uncertainties within the chemical manufacturing processes call for further investigation and industry transparency. Nonetheless, this work demonstrates the environmental benefits of tightened ODS feedstock regulations and underscores the importance of the HFC production phasedowns scheduled by the Kigali Amendment.

1 Introduction

When released into the atmosphere, chlorofluorocarbons (CFCs) contribute to stratospheric ozone loss while heating the earth's surface with radiative forcings thousands of times stronger than CO_2 on a centennial timescale [1]. Due to their ozone depleting potential (ODP), the production of CFCs for most uses is banned by the Montreal Protocol; accordingly, the atmospheric mixing ratios of the most abundant CFCs (e.g., CFC-11 and CFC-12) have declined in recent years, and there have been initial signs of ozone recovery [2, 3, 4, 5, 6]. However, the detection of unexpected sources of CFC emissions in recent years [7, 8, 9] has underscored the need to continually evaluate the consistency of reported values with atmospheric observations.

Ensuring compliance with the Montreal Protocol requires that unexpected emissions of controlled substances be carefully considered – which in turn requires a thorough assessment of emissions from permitted sources. For example, while CFC production for emissive uses has been banned globally since 2010, ongoing emissions of these gases from reservoirs produced prior to 2010, such as refrigerators and foams, continues to be a source of emissions [10]. The quantity of ODSs stored in these "banks" and the rate at which they are released have been the focus of recent work [11, 12, 13]. Additionally, there is an exemption for regulated CFCs to be produced and "entirely used" as feedstocks in the production of other compounds [14], such as hydrofluorocarbons (HFCs), with the requirement that this production is reported to the Ozone Secretariat of United Nations Environmental Program (UNEP) [14, 15, 16].

However, if a controlled substance is not isolated and is instead produced and consumed as part of a multi-step process in the same integrated chemical manufacturing facility, then it is considered an intermediate and reporting of its production is not required [15, 16]. Furthermore, controlled substances may be produced as unwanted by-products during the manufacturing of other compounds, but there is no reporting requirement for this production. Facilities are encouraged to maintain best practices to minimize by-products emissions [16], but certain production processes do yield "substantial emissions" of unwanted by-products [17], including the emission of CFC-115 during HFC-125 production [17].

In this work, we focus on recent atmospheric observations of CFC-113, CFC-114, and CFC-115 which indicate that there may have been sustained emissions of these compounds from 2004–2019 [18, 19, 20, 21, 22]. While the ozone depletion and surface warming caused by the emissions of minor CFCs from 2010–2020 has been estimated to be minimal, continued growth in emissions could negate some of the progress made by the Montreal Protocol [22], prompting further evaluation of these observations. Previous work has suggested that emissions from banked reservoirs of CFC-113, CFC-114, and CFC-115 cannot explain observationally-derived values [13], and while the portion of CFC-113, CFC-114, and CFC-115 emissions that cannot be accounted for by estimated bank emissions (i.e., the non-bank emissions) increased between 2004 and 2019 (Fig. 1A), the globally-aggregated feedstock production of CFC-113 and CFC-114 reported to the Ozone Secretariat decreased during this time (Fig. 1B; data from [23]). Thus, an unknown source of emissions may have contributed to atmospheric growth rates of these compounds.

Two possible explanations for these unexpected emissions are that either the chemical manufacturing pipeline that consumes CFC feedstocks became increasingly leaky or that feedstock reporting lagged actual feedstock production during this time. The Medical and Chemical Technical Options Committee's (MCTOC) 2022 Assessment Report estimated that improvements in emissions abatement technologies led to a decrease in feedstock emission rates from 4% (3–5%) in the 1980s to around 2.5% (0.9–4%) in the modern-day (not including emissions during transportation) [16], implying that under-reporting of feedstock production may be the more likely scenario. However, emission rates of feedstocks and by-products during the production of fluorinated greenhouse gases are "highly uncertain" and are thought to vary widely depending on factors specific to each manufacturing facility [24] – the 2019 Refinement to the 2006 IPCC Guidelines on National Greenhouse Gas Inventories suggested an emission factor of 4% with an uncertainty range of 0.1–20% [24] – so it is possible that global mean feedstock leakage rates have increased as older facilities have aged and new facilities have been built in regions with fewer regulations [25].

Regardless, these explanations both implicate the production of hyrdofluorocarbons (HFCs), which are the main end-products of manufacturing processes associated with CFC-113, CFC-114, and CFC-115 emissions [15, 16, 26]. In particular, the estimated growth of production of the refrigerants HFC-134a and HFC-125 from around 200 $\mathrm{Gg{\cdot}y^{-1}}$ in 2004 to 500 $\mathrm{Gg{\cdot}y^{-1}}$ in 2019 (shown in Fig. 1C–D; data from [25]) has been associated with the concurrent rise in a suite of CFC emissions [18, 19, 20, 22, 27]. However, these emissions have not been studied jointly or at a process level.

As is summarized in Fig. 2 (adapted from [23]) and described further in the Supplementary Note, there are multiple pathways for the production of HFC-134a and HFC-125 [26, 28, 29, 30], and the conversion efficiencies between feedstocks, intermediates, and end-products depend on the specific catalysts and reaction environments used [26]. These pathways are distinguished here by their unsaturated feedstocks, which are sequentially fluorinated into CFCs and/or hydrofluorinated into HCFCs and ultimately HFC end-products [26]. The allocation of production between these pathways is not publicly known, although it has been reported that the trichloroethylene (TCE) pathway, which may emit HCFC-133a but not CFCs, is more commonly used for HFC-134a production [31, 32, 33]. Recent reports on the atmospheric abundance of the intermediate compound HCFC-133a suggest that HFC-134a production by the TCE pathway may have increased since 2004, but the increase of observationally-inferred HCFC-133a emissions has not been consistent, and it is possible that emissions may be influenced by facility-level containment practices [21, 34]. For HFC-125, it was reported that 8 out of 12 production facilities in China used the tetrafluoroethylene (TFE) pathway [27], which is not known to emit CFCs as by-products, in 2011. However, it was also reported in 2023 that "most" HFC-125 was produced using PCE [17]. There is no known proxy for the TFE HFC-125 production pathway [29], so the usage of each production pathway cannot be inferred from observations. Given that the portion of each HFC produced by its corresponding production pathways determines feedstock, intermediate, and by-product generation, the unknown flow through the HFC production pipeline is a

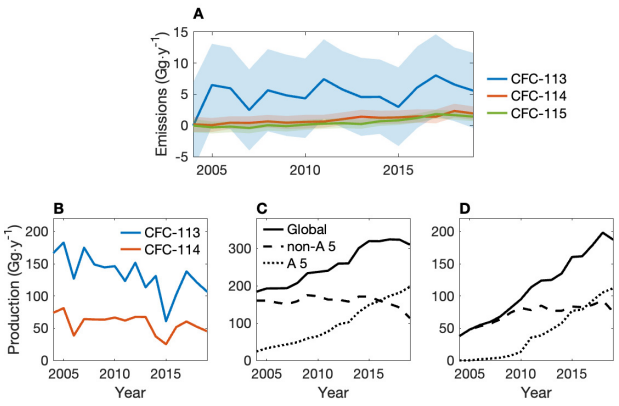

Figure 1: (A) The estimated portion of observationally-derived global emissions of CFC-113 (blue), CFC-114 (orange), and CFC-115 (green) that cannot be attributed to leakage from estimated banked reservoirs. (B) The globally-aggregated production of CFC-113 (blue) and CFC-114 (orange) for use as a feedstock, as reported to the Ozone Secretariat (no CFC-115 production was reported during this time; data from [23]). (C) HFC-134a and (D) HFC-125 estimated production globally (solid) and in A 5 (dotted) and non-A 5 countries (dashed) (data from [25]). In (A), the lines show median emissions, and the shaded regions encompass the 1-σ range of emissions based on emission model and bank uncertainties. Global emissions are derived using the AGAGE 12-box model [38, 61], and the calculation of bank emissions is described in the Methods.

key source of uncertainty in attributing CFC emissions to HFC production.

To date, emission rates have been estimated for each gas in isolation by calculating the ratio of observationally-inferred CFC emissions to HFC production [22, 35]. This, however, does not account for the balance between production pathways in the chemical manufacturing pipeline or the efficiency of conversion between intermediate products. As such, the sources of emissions (i.e., feedstocks, banks, and by-products) have not been comprehensively quantified, and reported feedstock and by-product emission rates [16, 24] have not been constrained with atmospheric observations. Quantifying these emission rates could inform future controls of the Parties to the Montreal Protocol and add to the environmental benefits (i.e., reduced surface warming and ozone depletion) attributable to the Kigali Amendment [25], which is estimated to avoid 0.4°C of warming by the end of the century through a phasedown of HFC production [7].

Here, we develop a probabilistic modeling approach, using Bayesian Parameter Estimation (BPE), that extends previous work [12] to jointly model CFC-113, CFC-114, and CFC-115 emissions from production, banks, use as feedstocks, and by-production as a function of their HFC-134a and HFC-125 end-products. (Unless otherwise noted, we refer to the sum of CFC isomers by the dominant isomer; i.e., CFC-113 refers to CFC-113+CFC-113a. Implications of this are discussed in the Methods.) We explicitly model HFC-134a production as the sum of two possible pathways (Fig. 2) and include observed HCFC-133a mixing ratios as an additional constraint on the relative production of HFC-134a through each pathway. (We chose HCFC-133a as a proxy for the TCE production pathway as HCFC-133a is the final intermediate of this pathway [26, 28]. Relative to HCFC-132b, HCFC-133a is also preferable in that it has a lower lifetime uncertainty and thus simulated mixing ratios are better constrained [21].) We do not include other HCFC intermediates as constraints for HFC-125 production as HCFC-123 and HCFC-124 have other known end-uses [26], and HCFC-122 may be used as an intermediate in their production. Previously reported estimates of HFC-134a and HFC-125 production in A 5 (low to middle income) and non-A 5 (high income) countries [25] are used to jointly model and constrain feedstock production and by-product emission rates from the manufacturing pipeline in the two classifications of countries. We draw on previously reported emission rates [16, 24], and production patents [26, 28, 36, 37] are used to inform conversion rates between feedstocks, intermediates, and their HFC end products. By explicitly modeling the conversion and by-production of these CFCs and HCFC-133a through the HFC-125 and HFC-134a manufacturing pipelines in A 5 and non-A 5 countries, we attempt to explain the apparent discrepancy between reported feedstocks and observationally-derived

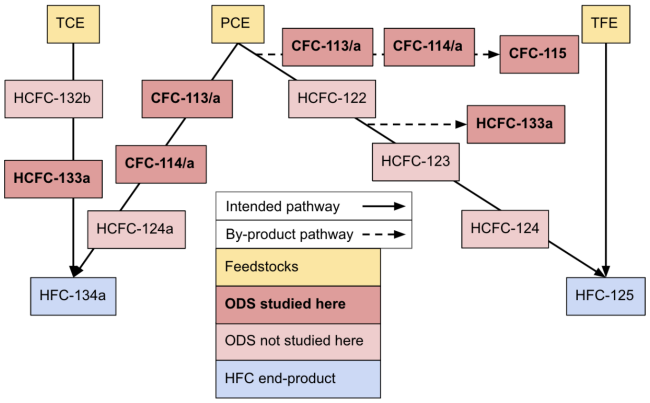

Figure 2: A schematic adapted from [23] of the known production processes for HFC-134a and HFC-125 according to relevant patents, as summarized in [26]. TCE = trichloroethylene, PCE = perchloroethylene, TFE = tetrafluoroethylene.

emissions and quantify feedstock and by-product emission rates in each country classification. Finally, we provide a lower-bound estimate of the unintended global warming and ozone depleting potential for recent HFC-125 and HFC-134a production, which quantifies the projected climate and ozone impact of their continued production under the Kigali Amendment.

2 Results

2.1 Simulated mixing ratios and emissions

The BPE posterior distributions of simulated CFC-113, CFC-114, CFC-115, and HCFC-133a surface mixing ratios accounting for emissions attributable to HFC production contain observations from 2004–2020 (Fig. 3, left column), confirming that our simulation model and parameter space are statistically consistent with observations. To quantify the impact of HFC production on observed mixing ratios, we compare BPE posterior mixing ratios with a scenario in which HFC-production-related emissions had not occurred from 2004–2019 (i.e., simulating mixing ratios using posterior emissions from non-HFC sources only). These results suggest that HFC production elevated the mixing ratios of CFC-113, CFC-114, and CFC-115 by 1.7 ppt (1.6–1.9 ppt), 0.79 ppt (0.70–0.90 ppt), and 0.57 ppt (0.52–0.61 ppt), respectively. We assume that HCFC-133a is only emitted during HFC-134a and HFC-125 production; therefore, due to its relatively short atmospheric lifetime, we estimate that the mixing ratio of HCFC-133a would have decayed to less than 0.01 ppt in 2020 had there been no HFC production throughout this time period.

Relative to previous work [13], the magnitudes and trends of the BPE posterior emission distributions for these gases provide an improved comparison with observationally-derived emissions from 2004–2019 (Fig. 3, right column). While it is apparent that the interannual variability in observationally-derived emissions cannot be explained by our results, several factors may contribute to this discrepancy. First, HFC production is informed partly by a top-down emission estimate, which cannot account for temporal misalignment in production and consumption and therefore may not capture the correct timing of production [25]. Next, our assumptions of constant emission rates from production cannot capture variability in facility-level emissions, such as leakage during maintenance or improvements to containment following modernization [34]. Finally, limitations in inferring emissions from surface observations may arise due to neglected variability in atmospheric transport [38], leading to the misinterpretation of variability in stratosphere-troposphere exchange as emissions fluctuations. These factors do not impact variability beyond interannual timescales and therefore do not impact our conclusions regarding emissions from 2004–2019.

The estimated contribution of each emission source is also shown in the right column of Fig. 3. (As CFC production for most end-uses was phased out by 2010, we combine emissions from production for non-feedstock use and banks here and refer to the sum as banks.) According to the BPE posterior distributions, bank emissions for CFC-113, CFC-114, and CFC-115 were approaching zero by 2019,

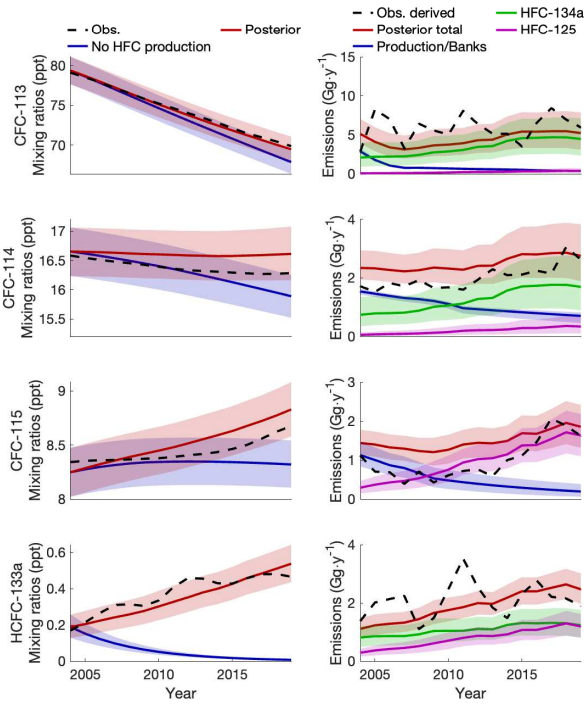

Figure 3: BPE posterior distributions of global mean surface concentrations (left column) and emissions attributable to the sources considered here (right column) for CFC-113 (top row), CFC-114 (second row), CFC-115 (third row), and HCFC-133a (bottom row). The dashed black lines are observations from AGAGE, and the colored lines and shaded regions are the median and 1-σ CI of each time series.

while HFC production drove the overall increases in total emissions, consistent with previous work associating HFC production to CFC and HCFC emissions [19, 20, 21, 22]. For CFC-113, our results attribute 76% (1-σ: 61–84%) of total emissions from 2004–2019 to HFC-134a production, including 86% (75–92%) from 2015–2019. In contrast, we estimate that HFC-134a production did not contribute a majority of annual CFC-114 emissions until 2012, although it did account for 62% (45–74%) of emissions from 2015–2019. Bank emissions were the largest source of CFC-114 prior to 2012, and they contributed 29% (21–40%) of emissions from 2015–2019. Our results also suggest that bank emissions were the dominant source of CFC-115 emissions through 2009, after which HFC-125 production dominated, including contributing 81% (68–92%) of emissions from 2015–2019. Finally, we estimate that 58% (53–68%) of HCFC-133a emissions from 2004–2019 were the result of HFC-134a production, with the remaining portion attributable to HFC-125 production, although these sources were statistically equivalent by 2019.

2.2 Emissions from HFC-134a production

As discussed above, HFC-134a can be produced via two different pathways, one of which consumes CFC-113 and CFC-114, while the other consumes HCFC-133a. Consistent with previous reports of the dominance of the TCE production pathway [31, 32, 33], which uses HCFC-133a, our BPE analysis suggests that this pathway accounted for 65% (49–80%) of global HFC-134a production from 2004–2019 (Fig. 4A). This percentage dropped as HFC-134a production grew in A 5 countries while decreasing in non-A 5 countries: We estimate that 59% (39–84%) of HFC-134a was produced via HCFC-133a in A 5 countries and 68% (45–89%) was produced via HCFC-133a in non-A 5 countries from 2004–2019.

As is shown in Fig. 4B–C, BPE estimated CFC-113 feedstock production grew from 114 Gg·y^{-1} (52–189 Gg·y^{-1}) in 2004 to 238 Gg·y^{-1} (144–322 Gg·y^{-1}) in 2019, while CFC-114 feedstock production grew from 102 Gg·y^{-1} (44–172 Gg·y^{-1}) to 214 Gg·y^{-1} (126–292 Gg·y^{-1}), and HCFC-133a production grew from 155 Gg·y^{-1} (109–194 Gg·y^{-1}) to 234 Gg·y^{-1} (182–292 Gg·y^{-1}). The estimated growth in the production of these compounds followed the growth in production of HFC-134a by the pathway

relevant to these compounds.

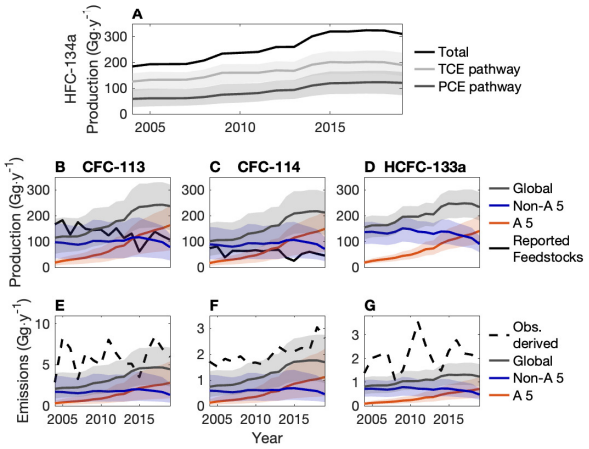

Figure 4: (A) Estimated global HFC-134a production (black; data from [25]) and the BPE estimated mass of HFC-134a produced using TCE (light gray) and PCE (dark gray) as feedstocks. BPE posterior distributions of (B–D) production and (E–G) emissions of CFC-113 (left), CFC-114 (middle), and HCFC-133a (right). The lines and shaded regions are the median and 1-σ CI, respectively, and in B–G, the gray, blue, and orange coloring denotes global, non-A 5, and A 5 countries, respectively. For reference, the mass of feedstock production reported to the Ozone Secretariat [23] is included in B and C, and the observationally-derived emissions are included in E–G.

To assess the efficacy of current reporting practices, we compare the globally-aggregated CFC-113 and CFC-114 feedstock production data reported to the Ozone Secretariat with our BPE estimated feedstock production (Fig. 4B–C). Notably, reported production values fall within our 1-σ interval for estimated non-A 5 production; given that reported values for CFC-113 came only from non-A 5 countries from 2008–2019 [15], this is an independent validation of our results. However, our results suggest that there is a large and growing portion of CFC-113 and CFC-114 feedstock production going unreported. Following from the previously reported estimate of HFC production in A 5 and non-A 5 countries used to inform our priors [25], 57% (35–80%) of CFC-113 and CFC-114 production occurred in A 5 countries from 2015–2019, up from 22% (9–47%) in 2004–2008, thereby increasing the portion of global feedstock production that was not reported.

Table 1: BPE posterior distributions of feedstock emission rates (FE in Eq. 2) for species used in the production of HFC-134a. Values are relative to inferred mass of feedstocks produced (see Fig. 4B–D). For global emission rates, the time mean of each percentile in the years 2015–2019 is taken. Median values are shown with 1-σ confidence intervals.

Species	Global	non-A 5	A 5
CFC-113	2.0% (1.3–2.8%)	2.0% (1.1–3.0%)	2.0% (1.1–3.0%)
CFC-114	0.8% (0.4–1.7%)	0.8% (0.4–1.3%)	0.9% (0.5–1.4%)
HCFC-133a	0.5% (0.3–0.8%)	0.6% (0.3–0.9%)	0.5% (0.3–0.9%)

BPE posterior distributions of the global emission rates of CFC-113, CFC-114, and HCFC-133a relative to inferred feedstock production are provided in Table 1. The emission rate distribution is highest for CFC-113 – 2.0% (1.3–2.8%) globally from 2015–2019 – while CFC-114 and HCFC-133a emission rates were 0.8% (0.4–1.7%) and 0.5% (0.3–0.8%), respectively. This CFC-113 emission rate estimate is at the low end of the MCTOC likely range of 1.5–6.2%, indicating that production facilities are operating as is expected for well-regulated modern facilities [16]. Based on our results, it is also possible that CFC-113 was not transported between production and consumption and therefore was not subject to the 0.3–1.2% emission rate that is expected during this step [16]. Meanwhile, the CFC-114 and HCFC-133a emission rates estimates were below the MCTOC range, suggesting that these compounds also may have not been transported between production and consumption and could

be considered intermediates without reporting requirements. For HCFC-133a, this is consistent with previous reports of it being a non-isolated intermediate in the production of HFC-134a [39].

Table 1 also provides estimated emission rates of CFC-113, CFC-114, and HCFC-133a in A 5 countries and non-A 5 countries. Contrary to previous assumptions that A 5 countries emit at a higher rate [40], the estimated non-A 5 and A 5 emission rates are not statistically different at the 1-σ confidence level. If our modeling assumptions are correct, this suggests that containment technologies are comparable across both sets of countries. As a result, the global feedstock emission rates have not changed as production has shifted to A 5 countries, and emissions in Fig. 4E–G have followed the same trends as inferred production.

Due to limited chemical conversion rates and the mass ratio between HFC-134a and its feedstocks, emission rates relative to HFC-134a production are higher than those relative to feedstock production itself. According to relevant patents and reports on the conversion processes [36, 37], approximately 98% of CFC-113 can be converted into CFC-114a and 94% of CFC-114a can be converted into HFC-134a. Meanwhile, the respective molar masses of CFC-113, CFC-114a, and HFC-134a are 187, 171, and 102 g mol^{-1} – therefore, about 2 g of CFC-113 could be needed to produce 1 g of HFC-134a. By dividing observationally-derived emissions of CFC-113 and CFC-114 by the BPE estimated mass of HFC-134a produced using the PCE pathway, our results suggest that the CFC-113 and CFC-114 emission rates relative to HFC-134a production from 2015–2019 were 4.0 wt% (2.6–5.4 wt%) and 1.5 wt% (0.9–2.2 wt%), respectively. An analogous calculation for the HCFC-133a emission rate relative to the estimated mass of HFC-134a produced by the TCE pathway suggests an emission rate of 0.7 wt% (0.4–0.9 wt%).

2.3 Emissions from HFC-125 production

Table 2: BPE posterior distributions of emission rates (BP in Eq. 2) for species produced as by-products in the production of HFC-125. Values are relative to the mass of HFC-125 produced (see Fig. 1D); percentages are therefore wt%. For global emission rates, the time mean of each percentile in the years 2015–2019 is taken. Median values are shown with 1-σ confidence intervals.

Species	Global	non-A 5	A 5
CFC-113	0.2% (<0.1–0.3%)	0.2% (<0.1–0.4%)	0.2% (<0.1–0.4%)
CFC-114	0.2% (<0.1–0.3%)	0.1% (<0.1–0.3%)	0.2% (<0.1–0.4%)
CFC-115	0.7% (0.5–1.0%)	0.8% (0.4–1.2%)	0.9% (0.5–1.4%)
HCFC-133a	0.7% (0.4–0.9%)	0.8% (0.4–1.1%)	0.5% (0.3–0.9%)

Given limited knowledge of by-product production, release, and destruction rates, it is not possible to determine the mass of by-products generated during HFC-125 production, so emission rates are reported in Table 2 relative to the mass of HFC-125 produced. Globally, the CFC-115 BPE estimated by-product emission rate was 0.7 wt% (0.5–1.0 wt%) from 2015–2019, which is consistent with the estimated range of 0.1–1 wt% recently reported by the UNEP's Technology and Economic Assessment Panel for this emission rate [17]. Following our modeling assumptions regarding the relative magnitude of CFC-115 emissions (see Methods; [17, 30]), the BPE estimated CFC-113 and CFC-114 emission rates (0.2 wt% (<0.1–0.3 wt%)) were lower than that of CFC-115. These rates are higher than what was recently reported based on plant data (<0.0001 wt%, [17]) but lower than the default emission factor of 4 wt% suggested by the 2019 Refinement to the 2006 IPCC Guidelines on National Greenhouse Gas Inventories [24].

Although the BPE estimated CFC-115 by-product emission rate is not inconsistent with UNEP's recent emission rate estimate, we expect our result to be biased low. As discussed above, it is not known how much HFC-125 is produced using the PCE pathway, which produces CFC-115 as a by-product, but it has been reported that only 4 out of 12 Chinese factories that produced HFC-125 in 2011 used this production pathway [27]. If global HFC-125 production follows the same ratio as Chinese factories, then the estimated CFC-115 emission rate would be 2–3 wt%, which would be closer to the 2019 Refinement to the 2006 IPCC Guidelines on National Greenhouse Gas Inventories value [24]. The BPE posterior emission rate of HCFC-133a, which does not have a specific previously estimated by-product emission rate, would also be within this 2–3 wt% range.

Table 2 shows that the BPE posterior HFC-125 by-product emission rates distributions are not

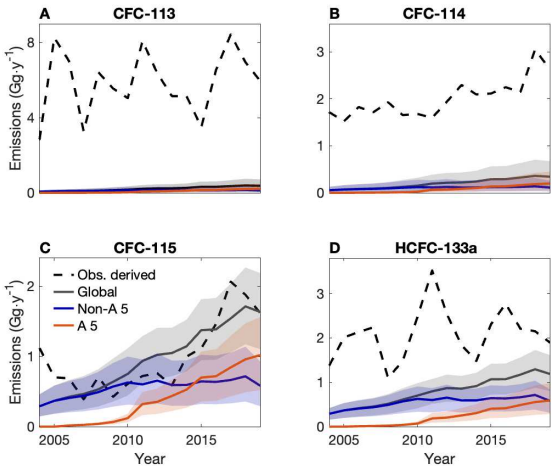

Figure 5: BPE posterior distributions of by-product emissions from the manufacture of HFC-125 for (A) CFC-113, (B) CFC-114, (C) CFC-115, and (D) HCFC-133a. Gray lines denote global emissions, while blue and orange lines denote emissions in non-A 5 and A 5 countries, respectively. Lines and shaded regions are the median and 1-σ CI, respectively, and observationally-derived emissions are included for reference.

higher in A 5 countries than in non-A 5 countries. Yet, despite the similarities in these rates, our results suggest that the rise in emissions from HFC-125 production from 2010-2019 was driven by an increase in production in A 5 countries. As is shown in Fig. 5, BPE estimated by-product emissions of CFC-115 and HCFC-133a from non-A 5 countries were flat during this time period, while emissions from A 5 countries followed the growth of HFC-125 production. Production of HFC-125 is expected to be dominated by A 5 countries in the coming decades [25], so improved technology for the separation and containment of unwanted by-products during the production of HFC-125 in A 5 countries may be needed to prevent future emissions of CFC-113, CFC-114, and in particular, CFC-115.

2.4 Ozone depletion and global warming potentials

While HFCs do not destroy ozone, the CFC and HCFC emissions considered in this analysis will do so. Per Gg of HFC-134a and HFC-125 produced, our results suggest that the ODPs of unintended ODS emissions were about 0.015 ODP-Gg (0.009–0.022 ODP-Gg) and 0.006 ODP-Gg (0.004–0.008 ODP-Gg), respectively, from 2015-2019.

Following from the increase in HFC-134a production, we estimate that the unintended ODP from HFC-134a production grew from 1.6 ODP-Gg·y^{-1} (0.8–2.9 ODP-Gg·y^{-1}) in 2004 to 3.5 ODP-Gg·y^{-1} (2.0–5.3 ODP-Gg·y^{-1}) in 2019 (Fig. 6A). This is consistent with the combined ODP of CFC-113 and CFC-114 feedstock emissions reported in Chapter 7 of the 2022 Scientific Assessment of Ozone Depletion (2.3–4.6 ODP-Gg·y^{-1}) [23]. Emissions of CFC-113, which has both the highest ODP of the ODSs considered here and the highest BPE estimated emission rate from HFC-134a production, account for 75% (64–83%) of the unintended HFC-134a ODP over this time period. For HFC-125, the unintended ODP is smaller, with a maximum of 1.2 ODP-Gg·y^{-1} (0.9–1.5 ODP-Gg·y^{-1}) in 2018 (Fig. 6B). By gas, we estimate that CFC-115 contributed 60% (46–74%) of HFC-125's unintended ODP from 2004–2019, while CFC-113 and CFC-114 contributed 20% (7–34%) and 16% (5–28%), respectfully. Emissions of HCFC-133a, which has a much lower ODP than any CFC, account for 0.8% (0.4–1.6%) and 3% (2–4%) of the ODP for HFC-134a and HFC-125, respectively. We estimate the total ODP of unintended emissions attributed to HFC-134a and HFC-125 production was 4.7 ODP-Gg·y^{-1} (3.1–6.3 ODP-Gg·y^{-1}) from 2015–2019, which is about 7% of the ODP of CFC-11 emissions during that time period [41].

By including the 100-year global warming potential (GWP) of unintended feedstock and by-product emissions, the total GWP attributable to HFC-134a and HFC-125 from 2004–2019 increases by 12% (7–18%) and 9% (6–11%), respectively (Fig. 6C–D). CFC-113 emissions from HFC-134a production had the largest GWP, which was 24.8 TgCO$_2$eq·y^{-1} (12.9–39.6 TgCO$_2$eq·y^{-1}) in 2019, while the 15.7

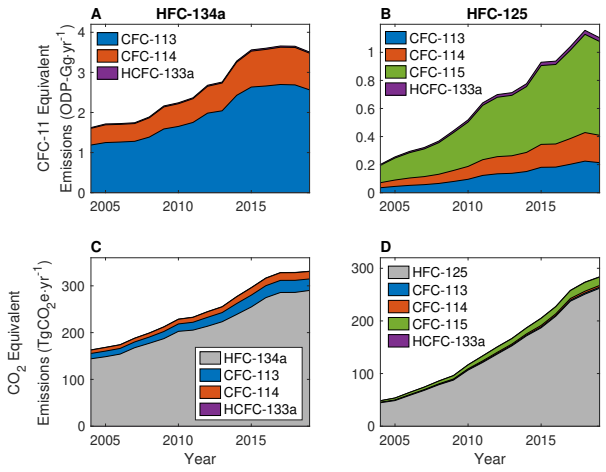

Figure 6: The (A, B) ODP and (C, D) GWP of emissions attributed to (A, C) HFC-134a and (B, D) HFC-125 production, with the blue, orange, green, and purple sectors representing the contributions of CFC-113, CFC-114, CFC-115, and HCFC-133a, respectively. HFC-134a and HFC-125 have no ODP and are therefore not included in A–B, while the GWP of HFC-134a and HFC-125 emissions are included for reference in C–D. GWP and ODP values were calculated with median emissions values; uncertainty ranges are presented in the text.

$TgCO_2eq{\cdot}y^{-1}$ (10.6–21.1 $TgCO_2eq{\cdot}y^{-1}$) of emissions of CFC-115 was the largest GWP of the HFC-125 by-products in 2019. The combined GWP of feedstocks and by-products of HFC-134a and HFC-125 was 62.5 $TgCO_2$-eq$\cdot y^{-1}$ (45.2–81.2 $TgCO_2$-eq$\cdot y^{-1}$) from 2015–2019 – which is equivalent to 0.2% of the approximately 36,000 $Tg{\cdot}y^{-1}$ of global CO_2 emissions during this time [42], increasing the total GWP attributable to HFC-134a and HFC-125 production to about 1.6% of global CO_2 emissions.

If future production of HFC-134a and HFC-125 maintain the same emission rates and allocation between respective production pathways, then the ODP and GWP estimated here will persist until production of HFC-134a and HFC-125 ends. By assuming that global emission rates and the the isomeric composition of emissions remain the same, we can estimate this future unintended ODP and GWP using the average of a recent HFC production projection that adheres to the Kigali Amendment [25], in which global HFC production peaks by the end of this decade and begins to decline around 2030. We project that unintended emissions of ODSs during HFC-134a production could result in a total of 79 ODP-Gg (50–107 ODP-Gg) and 910 $TgCO_2$-eq (574–1249 $TgCO_2$-eq) from 2020–2050, while HFC-125 production could result in 29 ODP-Gg (18–42 ODP-Gg) and 522 $TgCO_2$-eq (336–755 $TgCO_2$-eq). The estimated ODP and GWP of remaining halocarbons banks were about 3,600 ODP-Gg and 21,000 $TgCO_2$-eq in 2020 [13]; thus we estimate that unintended emissions from future HFC-134a and HFC-125 production could increase ODS contributions to ODP and GWP by 3% and 7%, respectively. If the CFC-emitting production pathways are eliminated, then the future ODP and GWP of HCFC-133a emissions from HFC-134a production would be 0.9 ODP-Gg and 16.7 $TgCO_2$-eq, while HFC-125 production could have no unintended ODP and GWP from the compounds considered here.

The ODP and GWP values presented here do not include the impacts of other feedstocks, intermediates, or by-products that are released during the production of HFC-134a and HFC-125. Two such compounds, HCFC-31 and HCFC-132b, have been detected in the atmosphere in small abundances (less than 0.2 ppt) leading to emission estimates of about 1 $Gg{\cdot}y^{-1}$ of each. These compounds have ODPs of 0.019 and 0.038, respectively, and GWPs of 85 and 332, respectively; therefore, the total ODP and GWP of emissions related to HFC-134a and HFC-125 production is higher by about 1% due to these HCFCs. A full life-cycle analysis of HFC-134a and HFC-125 is outside of the scope of this work, but the contribution of CCl_4, which is a feedstock for PCE production, would need to be considered to capture the full ODP and GWP of these HFCs.

3 Summary and Discussion

3.1 Montreal Protocol reporting practices fall short in capturing increased CFC production

By jointly modeling the emissions of CFC-113, CFC-114, CFC-115, and HCFC-133a from reported non-feedstock production and from HFC-134a and HFC-125 production, we find that the increase in non-bank emissions of CFC-113, CFC-114, and CFC-115 from 2004–2019 can be explained by the concurrent increase in HFC production. In particular, we find that the use of CFC-113 and CFC-114 as feedstocks or intermediates during the production of HFC-134a and the undesirable production of CFC-115 in a side reaction during the production of HFC-125 were likely the dominant sources of emissions for these compounds. Additionally, we find that HCFC-133a emissions during this time came primarily from its use as an intermediate in the production of HFC-134a, although the increase in emissions from 2004–2019 may have been driven by undesirable by-production during the manufacturing of HFC-125.

Our results suggest that recent reporting of feedstock production is not sufficient to account for the production and emission of CFC-113, CFC-114, and CFC-115. From 2008–2019, A 5 countries did not report feedstock production of CFC-113, although some quantity of this compound is thought to be produced in these countries for use as a feedstock [15]. If our modeling assumptions are correct, then our results would suggest that CFC-113 (and CFC-114) were likely produced in increasing quantities in A 5 countries for use in HFC-134a production. Meanwhile, our estimated production of CFC-113 and CFC-114 for use as HFC-134a feedstocks in non-A 5 countries was consistent with reported feedstock production values for these compounds, which were not used to inform our model. Assuming that non-A 5 feedstock reporting is accurate, this consistency provides some external validation of our modeling results. From 2015–2019, we estimate that A 5 countries accounted for 61% (33–86%) of CFC-113 and CFC-114 production, and the fraction of production occurring in A 5 countries will grow as global HFC production continues to shift to that part of the world. Thus, if reporting practices persist, we expect that the unreported fraction of CFCs used in manufacturing HFCs will continue to grow.

It has previously been suggested that the non-reporting of CFC-113 production in A 5 countries indicates its use as an intermediate, rather than a feedstock, in the production of other fluorinated compounds [15]. This distinction has practical implications for emissions – intermediates should be emitted at a lower rate – and regulatory implications for whether or not production is required to be reported under the Montreal Protocol. Due to the magnitude of uncertainty in our results relative to the precision needed to differentiate between use as a feedstock and intermediate, we cannot definitively say whether CFC-113 and CFC-114 were produced and consumed as intermediates or feedstocks. However, assuming that the HFC-134a production estimate used here is accurate and that non-A 5 countries produced and consumed feedstocks in separate processes, results from our analysis suggest that A 5 countries have either not fulfilled their reporting obligations or have facilities that emit at a higher rate than non-A 5 facilities. The latter assumption is supported by the consistency between reported CFC-113 and CFC-114 feedstock production and our model-inferred feedstock production values in non-A 5 countries – reporting would not have been required if production and consumption occurred in the same integrated process. If all steps in the production process emit at the same rate across the globe, then emissions from processing and transport are required for A 5 emission rates to match non-A 5 emission rates. Conversely, if CFC-113 and CFC-114 are produced and consumed as part of an integrated production process in A 5 countries, then some other part of the production process must emit at a higher rate to compensate for the 0.3–1.2% emission rate that occurs during transportation [16]. If our modeling assumptions are correct, then A 5 countries either need to report feedstock production or improve emission containment to match that of non-A 5 countries. However, we note that our results are contingent on our assumptions regarding of HFC production totals, the distribution of production between A 5 and non-A 5 countries, and the relative utilization of each production pathway, which represent critical sources of uncertainty that cannot be resolved in the present modeling framework.

3.2 Lingering uncertainty

The assumptions underlying our simulation of CFC emissions from HFC production are informed by published patents and estimated HFC production data. Nonetheless, biases in these assumptions would affect our results; thus, our analysis is limited by a lack of insight into industrial processes. For example,

we assume that chemical conversion rates are at the high end of reported values. Yet if chemical conversion rates were lower – in line with those reported by a recent review of fluorinated refrigerants [26] – then our estimated CFC-113 feedstock production would be higher, while the estimated CFC-114 feedstock production would be lower, bringing both in closer agreement with reported values (see Supplementary Fig. 1). It is also possible that a temporal increase in conversion rates could account for some portion of the decrease in reported feedstock production, but we do not account for changes in conversion rates in our model. Therefore, the chemical conversion rates are a key source of uncertainty that cannot be resolved without further transparency from the chemical manufacturing industry. Additionally, given that we do not have observable proxies for both HFC-125 production pathways, we cannot evaluate which pathway was used or whether temporal or geographic variability in pathway usage contributed to apparent increases in by-product emissions. In particular, the sharp increase in observationally-derived CFC-115 emissions around 2012 could be explained by a shift in production towards the PCE pathway, which produces CFCs as unwanted by-products. This would be consistent with the shift from 4 out 12 Chinese factories using the PCE pathway in 2011 [27] to "most" global factories using this pathway in 2023 [17], but this cannot be confirmed without industry knowledge.

Without additional industry knowledge, it also remains possible that the emissions of CFCs from HFC production are very small, and that the non-bank emissions that we are concerned with come from an unrelated process. In our results, we show that it is possible for HFC production to explain CFC-113, CFC-114, and CFC-115 emissions, but we do not include a term for "unknown or unrelated production" in our simulations, and the previously reported values that inform our priors include combinations of emission and conversion rates that allow HFC production to explain CFC-113, CFC-114, and CFC-115 observations. Previous reports suggest that the large majority of reported CFC-113 produced for use as a feedstock ended up as HFC-134a [15], but this is a qualitative statement that could quantitatively change over time, and given that A 5 countries did not report CFC-113 production, this only pertains to non-A 5 countries. If HFCs are entirely produced by non-CFC production pathways in A 5 countries, then HFC production is not sufficient to explain recent CFC observations and another source of emissions must exist. In particular, recent production of chlorotrifluoroethylene (CTFE) plastics, trifluoroacetic acid (TFA), and the hydrofluoroolefin HFO-1336mzz(Z) were likely to have used CFC-113 or CFC-113a as a feedstock or intermediate [15, 43, 44]. We assume that emissions from those production processes are negligible here, but future work may have to consider them as the production of those end-products grows.

Uncertainty in global emissions of these compounds and their emission rates also arises from the compounds' lifetimes, which are inversely proportional to emissions in top-down estimates [38]. Observationally-derived emissions and simulated mixing ratios were both calculated here using the median of a previously reported "most likely" lifetime range [45], but different methods for calculating lifetimes yield values that are at least 10% longer or shorter than the lifetimes used here [12, 38, 45, 46]. We test the sensitivity of our model results to CFC lifetimes by simulating mixing ratios using a range of lifetimes informed by previous work, as described further in the Supplementary Methods. By doing so, we find that BPE posterior emission rates from feedstock production vary between 1.8% (1.1–2.6%) and 2.2% (1.5–2.9%) for CFC-113 and between 0.7% (0.3–1.6%) and 0.9% (0.5–1.7%) for CFC-114, and the BPE posterior emission rate for CFC-115 from HFC-125 production varies between 0.7 wt% (0.5–1.0 wt%) and 0.8 wt% (0.5–1.0 wt%). Thus, estimated feedstock and by-product emission rates vary within the 1-σ range of estimated uncertainty as the atmospheric lifetimes of these compounds vary within our prescribed range of lifetimes, and adopting these different lifetime values does not qualitatively change the conclusions regarding feedstock reporting.

A final caveat to the assumption that CFC-113 and CFC-114 emissions come from HFC-134a production is that only the minor isomer of CFC-114 (CFC-114a) is required for HFC-134a production. CFC-114a can be produced from CFC-114, or it can be produced directly from CFC-113 or CFC-113a, thereby avoiding the major isomer [26, 47]. Thus, it is possible for CFC-114a to be the only isomer emitted during the production of HFC-134a. Yet, CFC-114a emissions alone cannot explain the increase in the emissions of the sum of the two isomers, so some amount of CFC-114 must be produced and emitted, either as part of the HFC-134a production process or elsewhere. It is also possible that CFC-113a is avoided in the production of HFC-134a (if CFC-113 is converted directly into CFC-114a [47]), but we assume this is unlikely given the enhancement of both CFC-113a and CFC-114a measured in air samples collected downwind of a region where HFC-134a is produced in China [18].

4 Conclusion

We have developed a Bayesian method that jointly models the production and emission of CFC-113, CFC-114, CFC-115, and HCFC-133a during the chemical manufacturing of HFC-134a and HFC-125. In our model, unintended emissions from these manufacturing processes are able to explain the recent observations of CFC-113, CFC-114, CFC-115, and HCFC-133a that appear inconsistent with reported production of these compounds. If our assumptions are correct, then this indicates that a growing share of feedstock production is going unreported (possibly due to being considered an intermediate), largely in A 5 countries. We also infer emission rates from facilities around the world that are consistent with best practices, but the added ozone depletion and surface warming potential of these unintended emissions will have to be considered when estimating the total impact of future HFC production nonetheless. This work prompts a broader consideration of the use of regulated substances as feedstocks, including CCl_4, and enhances the benefits of compliance with the Kigali Amendment.

Methods

We extended a previously developed Bayesian model [12, 13] to jointly estimate the production for non-feedstock end-uses, banks, feedstock usage, emissions, and mixing ratios of CFC-113, CFC-114, CFC-115, and HCFC-133a. The modeling approach uses Bayesian Parameter Estimation (BPE), a form of Bayesian analysis which allows us to apply inference to a deterministic simulation model [48, 49]. In earlier iterations of the BPE model, the production priors were modeled independently across compounds [12, 13]. Here, we have updated the BPE model to explicitly model feedstock production and by-product generation as a function of relevant HFC production in A 5 and non-A 5 countries, thus differentiating emissions by region and accounting for inter-dependencies between the production of these molecules in the manufacturing pipeline.

The BPE model is implemented using the following steps. First we specify a simulation model of production, banks, emissions, and mixing ratios to jointly represent the manufacturing and emission processes impacting the suite of compounds in our analysis (Eqs. 1–6). Next, we develop prior distributions for most of the input parameters to reflect published estimates and their corresponding uncertainties. We then sample from the prior distributions and run the simulation model to obtain a joint distribution of output parameters, including banks, emissions, and mixing ratios. And finally, using Bayes' Rule, we jointly update both input and output parameters given observed mixing ratios of CFC-113, CFC-114, and CFC-115 from 1990–2020 and observed mixing ratios of HCFC-133a from 1990–2019. The methods are provided in more detail below.

Bayesian Parameter Estimation Model

Mixing ratios ($M_{i,t}$) for compound i in time t are simulated as

$$M_{i,t+1} = M_{i,t} * e^{-\tau_i^{-1}} + A * E_{i,t}, \tag{1}$$

where A is a constant that converts the mass of emissions (Gg) into mixing ratios (ppt) and accounts for the discrepancy between surface and global mean atmospheric mixing ratios [10]. Previously reported atmospheric lifetimes (τ_i) of 93, 191, 540, and 4.6 years were used for CFC-113, CFC-114, CFC-115, and HCFC-133a, respectively [45, 50]. The lifetimes for CFC-113 and CFC-114 used here are for the dominant isomer of these compounds and therefore overestimate the total lifetime of the sum of the isomers (lifetimes of CFC-113a and CFC-114a are 55 and 105 years, respectively [51]). If the atmospheric abundance of minor isomers was significant, then posterior estimates would be biased towards simulations with lower total emissions. However, atmospheric mixing ratios of CFC-113a and CFC-114a were 1.0 ppt and 1.1 ppt in 2020 [22], while atmospheric mixing ratios of the sum of CFC-113 and CFC-114 isomers were 69.4 ppt and 16.3 ppt, respectively [52], so we assume this bias is small.

To simulate the emissions time series used in Eq. 1, we summed the four emission sources that we assume comprise the total emissions of each compound. These include emissions from: production for non-feedstock use ($Prod_{i,j,t}$, where j denotes the application type), banks ($B_{i,j,t}$), use as a feedstock in HFC-134a production ($FS^k_{i,t}$, where k denotes use in A 5 or non-A 5 countries), and generation as a by-product during the manufacturing of HFC-125 ($HFC125^k_t$). Note that $Prod_{133a,j,t} = 0$ and $B_{133a,j,t} = 0$ for all t, as production of HCFC-133a was not reported. In addition, $FS^k_{115,t} = 0$ for all

t, as CFC-115 is not used as a feedstock in manufacturing HFC-134a. For each non-feedstock end-use, the fraction of production emitted directly (i.e., the direct emission rate) is denoted by $DE_{i,j}$ and the fraction of the bank released each year (i.e., the release fraction) is denoted by $RF_{i,j}$. Feedstock and by-product emission rates for each country classification are denoted by FE_i^k and BP_i^k. Thus, the emission time series for each compound is calculated as

$$\begin{aligned} E_{i,t} =& \Sigma_{j=1}^{N_1}(DE_{i,j} * Prod_{i,j,t} + RF_{i,j} * B_{i,j,t}) \\ &+ \Sigma_{k=1}^{N_2}(FE_i^k * FS_{i,t}^k + BP_i^k * HFC125_t^k), \end{aligned} \tag{2}$$

where direct and bank emissions are summed over N_1 equipment types (i.e., long and short banks), and feedstock and by-product emissions are summed over N_2 country classifications (i.e., A 5 and non-A 5).

Banks are simulated recursively for each equipment type as

$$B_{i,j,t+1} = (1 - RF_{i,j}) * B_{i,j,t} + (1 - DE_{i,j}) * Prod_{i,j,t}, \tag{3}$$

and feedstock production in each country classification is calculated as

$$\begin{aligned} FS_{114,t}^k =& M_{114}/M_{134a} * \chi_t^k * HFC134a_t^k \\ &* 1/(C_{114\to134a} * (1 - FE_{114}^k)), \end{aligned} \tag{4}$$

$$\begin{aligned} FS_{113,t}^k =& M_{113}/M_{114} * FS_{114,t}^k \\ &* 1/(C_{113\to114} * (1 - FE_{113}^k)), \end{aligned} \tag{5}$$

$$\begin{aligned} FS_{133a,t}^k =& M_{133a}/M_{134a} * (1 - \chi_t^k) * HFC134a_t^k \\ &* 1/(C_{133a\to134a} * (1 - FE_{133}^k)), \end{aligned} \tag{6}$$

where M_k is the molar mass of compound k, χ_t^k is the fraction of HFC-134a produced via the PCE pathway (which may emit CFC-113 and CFC-114), and $C_{a\to b}$ is the conversion rate from compound a to compound b. χ_t^k thus represents the dependencies between CFC-114 and HCFC-133a feedstock production, and $C_{113\to114}$ represents dependencies between CFC-113 and CFC-114 feedstock production in the deterministic simulation model.

Prior distributions

Non-feedstock production priors, $Prod_{113,j,t}$, $Prod_{114,j,t}$, and $Prod_{115,j,t}$ were developed for years prior to 1989 using production data reported to Alternative Fluorocarbons Environmental Acceptability Study (AFEAS) [53]. For CFC-113, this data was augmented according to the WMO (2003) correction [46], and total production data from 1989–2016 were taken from the WMO 2022 report on production and consumption of ozone depleting substances [23]. We assume no production following the end of reporting. For CFC-114 and CFC-115, total production data from 1989–2003 were taken as the greater of AFEAS data or AFEAS data scaled to match WMO production data, and total production data from 2004–2019 were taken from WMO's 2022 report [23]. To account for uncertainty in reported production, we assume lognormal distributions for $Prod_{113,j,t}$, $Prod_{114,j,t}$, and $Prod_{115,j,t}$, following previous work [11], where we assume the bias in reported data has a correlation term, $\rho_{i,j}$, that we infer in the BPE model (see [11] for more details). We set lower bounds of these distribution as 70%, 95%, and 80% of reported values, respectively, to ensure that observed mixing ratios were within the simulated priors [12]; see [11] for further description of these distributions.

The allocation of production to short or long bank equipment types for CFC-113 and CFC-114 was informed by AFEAS data when available and fixed to values from the final year of AFEAS data afterwards. Given the poor fit between simulated mixing ratios and observations that was previously reported for CFC-115 [13], we set the fraction of CFC-115 production allocated to short banks as an uncertain parameter with a prior uniform distribution between 50–90%. This uncertain parameter reflects uncertainty in AFEAS production allocation for CFC-115 – only production for refrigeration (i.e., long bank) was reported to AFEAS, but CFC-115 was also used as an aerosol propellant (i.e., short bank) [54], though this was not documented in AFEAS data. The addition of this parameter

resulted in an improved fit between posterior simulated mixing ratios and observations (Supplementary Fig. 2), so we continued with this altered end-use allocation.

Production of HFC-134 and HFC-125, $HFC134a_t^k$ and $HFC125_t^k$, from 1990–2019 were taken from a previously reported joint bottom-up and top-down estimate [25] and were assumed to be 0 prior to 1990. These data are calculated using data from several sources, including consumption reported by non-A 5 countries to the United Nations Framework Convention on Climate Change [55], previously estimated Chinese and Indian consumption estimates [56, 57], and emissions inferred from AGAGE [58] and National Oceanographic and Atmospheric Administration (NOAA) Global Monitoring Laboratory [59] observations of surface mixing ratios. Values are reported for A 5 and non-A 5 countries, thereby allowing for separation of production from the two classifications in our simulations. Note that we do not account for uncertainty in HFC production in our model, as uncertainties in the FE_i^k and BP_i^k terms in Eq. 2 and χ_i^k term in in Eqs. 4 and 6 and would linearly compensate for biases in HFC production. Nonetheless, we note the posterior distributions of these terms are conditional on the adopted HFC production time series.

Prior distributions of $DE_{i,j}$ and $RF_{i,j}$ were specified for each non-feedstock end-use based on industry-reported data [60], following recent work [12]. FE_i^k distributions were informed by the range of likely values reported by MCTOC [16] (1.5–6.2%). For computational efficiency, after simulating each gas independently, the FE_i^k parameter space was updated to remove the tails of the parameter space where the conditional probability of the data given the parameter value was near zero. FE_i^k was also adjusted to include values less than 1.5%. BP_i^k distributions were informed by a recent patent for HFC-125 production that reports by-product generation rates relative to HFC-125 production [30], with maximum emission rates of 2% and 1.5% for CFC-115 and HCFC-133a, respectively, and CFC-113 and CFC-114 emission rates of no more than half of the CFC-115 emission rate. We do not know how much of each by-product is emitted (as opposed to captured and/or destroyed), so we assumed beta distributions with parameters (2, 2) for FE_i^k, BP_{115}^k, and BP_{133a}^k priors and uniform distributions between 0–0.5 $* BP_{115}^k$ for BP_{113}^k and BP_{114}^k priors. Previous work has assumed that emission rates from chemical manufacturing are higher in A 5 countries than in non-A 5 countries [40]; to explore this possibility, we specify independent but identical priors for FE_i^k and BP_i^k for A 5 and non-A 5 countries.

Following a series of patents in which the chemical conversion rates of CFC-113 to CFC-114, CFC-114 to HFC-134a, and HCFC-133a to HFC-134a are reported under various conditions [26, 28, 36, 37], $C_{113\rightarrow114}$ $C_{114\rightarrow134a}$, and $C_{133a\rightarrow134a}$ were set to fixed values of 98% and 94%, and 95%, respectively. Although we do not know which catalysts and reaction conditions are used, we assume that conversion rates are at the high end of reported values based on the assumption that this is a mature industry where manufacturers would want to minimize unused resources. We set these as fixed values as the technology for these chemical conversion processes is not known to have changed with time. Simulations run with lower conversion rates suggest greater feedstock production, but this does not qualitatively change our conclusions (i.e., inferred under-reporting of CFC-113 feedstock production is increased when conversion rates are lowered, so our choice of conversion rates makes our unreported feedstock results conservative). Prior distributions for FE_i^k, BP_i^k, and $C_{a\rightarrow b}$ are summarized in Table S1.

χ^k was assumed to be a uniform distribution between 0–70%, based on previous reporting that the TCE pathway is more commonly used for HFC-134a production [31, 32, 33]. This prior incorporates an autocorrelation term that is sampled from a uniform distribution between 0.95–1.0 to reflect the potential for gradual change to global manufacturing.

As the initial year of reporting varies, we start our simulation model in 1955 for CFC-113, 1935 for CFC-114 and CFC-115, and 1990 for HCFC-133a. Initial mixing ratios are assumed to be 0 for CFCs and 0.0489 ppt for HCFC-133a [34]. As available production data for our bottom-up emissions estimates end in 2019, we implement the simulation model out to 2020.

Likelihood function

As in previous work [12], the difference between modeled and observed mixing ratios was assumed to be normally distributed with a mean of zero. Therefore, the likelihood function is a multivariate normal likelihood function of the difference between modeled and observed mixing ratios:

$$P(D_i|\theta) = \frac{1}{\sqrt{(2\pi)^{N_{obs}}|\Sigma_i|}} e^{(-\frac{1}{2}\epsilon_i^T \Sigma_i^{-1} \epsilon_i)}, \tag{7}$$

where D_i is a vector of annual global mean observed mixing ratios for each year from 1990–2020, N_{obs} is the length of D_i ($N_{obs} = 31$ for CFCs and 6 for HCFC-133a, see below), θ is the vector of all input and output parameters from the simulation model, ϵ_i is an N_{obs}x1 vector of the difference between modeled and observed mixing ratios in each year with a temporal covariance matrix Σ_i.

Within the error covariance matrix, we assumed additive error in uncertainties for each compound. Therefore, Σ_i contains the sum of the uncertainties in observed and simulated mixing ratios along its diagonals with the off-diagonals autocorrelated with coefficient of 0.95, representing an expected high autocorrelation in error for both the observed and simulated mixing ratios. Based on uncertainties in measurements and the relationship between surface point observations and global mean mixing ratios, CFC-113, CFC-114, and CFC-115 global mixing ratios have uncertainties of 1.5%, 3.0%, and 3.0%, respectively [38]. The uncertainty in the simulation model is not known, and due to computational limitations, sampling model uncertainties in the joint BPE model was not feasible. We therefore iteratively selected model uncertainties for each compound by initially specifying a prior model uncertainty error as a function of observed mixing ratios. We then ran the BPE model for each compound independently and selected the most likely model uncertainty term, with a precision of 0.5% of observed mixing ratios. This resulted in total uncertainties of 3.0% of observed mixing ratios for CFC-113 and 4.0% for CFC-114 and CFC-115. For HCFC-133a, measurements had an estimated 2-σ uncertainty of 10% [34], and given that our assumptions do not capture variability in industrial practices that have previously been hypothesized to result in variability in HCFC-133a emissions [21], we aggregated the observational data into five-year annual means and adopted a total uncertainty of 20% of observed mixing ratios for HCFC-133a. As the autocorrelation term is uncertain, we modeled it as a beta distribution between 0.6–0.8 with parameters (2, 2). We tested the sensitivity of our results to the model uncertainties by evaluating the likelihood function with uncertainties 50% smaller and 25% larger than those listed here, and the results were not qualitatively impacted.

Global mean mixing ratios were estimated by the AGAGE 12-box model of atmospheric transport [38, 61] using measurements taken by the AGAGE surface observation network [27, 58]. HCFC-133a data were taken from a previously published work [21] that followed this method.

We tested the robustness of our results to a different observational dataset for CFC-113 from the NOAA network [59] in place of AGAGE observations. CFC-114, CFC-115, and HCFC-133a are not measured by the NOAA network and therefore were unchanged in this sensitivity test. Posterior estimates of feedstock and by-product emission rates calculated with AGAGE and NOAA datasets are within 1-σ uncertainty (Table S2), indicating that our results are not specific to our choice of observational data.

Estimation of posterior distributions

To estimate the joint posterior distributions of the input and output parameters of Eqs. 1–6, we implement Bayes' Rule:

$$P(\theta|D_{113}, D_{114}, D_{115}, D_{133a}) \propto P(\theta)P(D_{113}|\theta)P(D_{114}|\theta)P(D_{115}|\theta)P(D_{133a}|\theta), \tag{8}$$

where θ denotes the input and output parameters of the deterministic simulation model (Eqs. 1–6), and thus $P(\theta)$ denotes the joint prior distribution of the input and output parameters. D_i denotes the observed mixing ratios of molecule i. As in previous work [12], we assume that the data (D_{113}, D_{114}, D_{115}, D_{133a}) are conditionally independent given θ, and that $P(D_i|\theta)$ is the multivariate likelihood function of all years of observed mixing ratios for molecule i given θ. In addition, for computational efficiency, Eq. 8 is estimated through sequential Bayesian updating in three steps. We first update the input parameters given D_{115}:

$$P(\theta|D_{115}) \propto P(\theta)P(D_{115}|\theta). \tag{9}$$

The posterior $P(\theta|D_{115})$ distribution is then used as the prior and updated given D_{114} and D_{133a}:

$$P(\theta|D_{114}, D_{115}, D_{133a}) \propto P(\theta|D_{115})P(D_{114}|\theta)P(D_{133a}|\theta). \tag{10}$$

This posterior is then updated once more given D_{113} to obtain the full joint posterior:

$$P(\theta|D_{113}, D_{114}, D_{115}, D_{133a}) \propto P(\theta|D_{114}, D_{115}, D_{133a})P(D_{113}|\theta). \tag{11}$$

For further description on the implementation of the BPE model, see [12].

The posterior distribution was estimated using the sampling importance ratio (SIR) method [49, 62, 63], which involves first sampling the prior distributions and then resampling the prior samples at a rate proportional to the importance ratio, which is proportional to the likelihood function defined in the previous subsection. As noted previously, we implement SIR through sequential updating. To do so, we first solve Eq. 9 by sampling 2,000,000 samples from θ's prior distribution and run the simulation model for CFC-115. Note that for computational efficiency in the first iteration of sequential updating, we only sample the parameters that are used in the CFC-115 simulation model. We then resample 1,000,000 samples from these prior samples, proportional to each sample's importance ratios, given by

$$\frac{P(\theta|D_{115})}{P(\theta)} \propto P(D_{115}|\theta). \tag{12}$$

Of all the parameters in the CFC-115 simulation model conditionally dependent on D_{115}, BP^k_{115} is the only one that informs priors for CFC-113 and CFC-114, and thus HCFC-133a as well. In the second iteration of sequential updating, the posterior samples of BP^k_{115} are used to inform the priors of BP^k_{113} and BP^k_{114}. For all other parameters in θ used in the CFC-114 and HCFC-133a simulation models, we sampled from their priors 1,000,000 times and ran the simulation model for CFC-114 and HCFC-133a. All 1,000,000 samples (i.e., both the updated parameters from the CFC-115 simulation and the prior samples from CFC-114 and HCFC-133a) were then resampled 300,000 times, proportional to the importance ratio:

$$\frac{P(\theta|D_{115}, D_{114}, D_{133a})}{P(\theta|D_{115})} \propto P(D_{114}|\theta)P(D_{133a}|\theta). \tag{13}$$

In the final sequence of updating, the FS^k_{114} posterior is used to inform the FS^k_{113} prior (Eq. 5). We drew 300,000 samples from all remaining parameters in θ and ran the CFC-113 simulation model. Finally, to obtain the full joint posterior distribution, all 300,000 samples (i.e., the updated parameters from the CFC-114, CFC-115, and HCFC-133a simulations and the prior samples from the CFC-113 simulation) are resampled 100,000 times proportional to the importance ratio:

$$\frac{P(\theta|D_{115}, D_{114}, D_{133a}, D_{113})}{P(\theta|D_{115}, D_{114}, D_{133a})} \propto P(D_{113}|\theta). \tag{14}$$

Ozone depletion and global warming potentials

To quantify how HFC-134a and HFC-125 production may delay the healing of the ozone layer and warm Earth's surface, we calculated the ozone depleting potential (ODP) and 100-year global warming potential (GWP) of the emissions attributed to the production of these compounds. HFCs do not contribute to ozone destruction, so the ODP of unintended feedstock and by-product emissions constitutes the entire ODP attributable to HFC-134a and HFC-125. For GWP, we included the contribution of HFC-134a and HFC-125 emissions [25] (GWPs of 1300 and 3170, respectively). These observationally-derived emissions estimates can only account for what has been emitted (either directly from the production process or from banks) and cannot capture the GWP of HFCs currently banked that may leak from their current reservoir until the end of their equipment's life.

For CFC-113 and CFC-114, which each had two isomers emitted from 2004–2019, we weighted ODPs and GWPs based on the recently reported isomeric composition of emissions. Emissions of the minor isomers, CFC-113a and CFC-114a, averaged 2.0 Gg·y^{-1} and 0.45 Gg·y^{-1} from 2004–2019 [22], respectively, making them both roughly 40% of the total CFC-113 and CFC-114 emissions. Using previously reported ODPs of 0.82, 0.73, 0.53, and 0.72 and GWPs of 6530, 3930, 9450, and 7410 for CFC-113, CFC-113a, CFC-114, and CFC-114a [64], respectively, we calculated weighted ODPs and GWPs of 0.78 and 0.61 and 5490 and 8634 for CFC-113 and CFC-114, respectively. For CFC-115 and HCFC-133a, we used previously reported ODPs of 0.45 and 0.019 and GWPs of 9630 and 378 [64]. We report ODP in units of ODP-Gg, which is the mass-weighted equivalent emissions of CFC-11, and we report GWP in units of $TgCO_2eq$, which is the mass of CO_2 that would result in the same radiative forcing on a 100-year time scale.

Data and Code Availability

All mixing ratio, production, and emissions data, as well as code for Bayesian analysis and plots, are available through Zenodo (https://doi.org/10.5281/zenodo.12207950).

Acknowledgements

The authors would like to acknowledge support from VoLo foundation. M.J.L. would like to acknowledge support from the Atmospheric Chemistry Division of the National Science Foundation (grant no. 2128617). The authors would also like to thank Luke Western for providing output from the AGAGE 12-box model, as well as Susan Solomon and Stefan Reimann for helpful discussions.

Author Contributions

Both authors conceptualized the work and developed the methods. SB conducted the analysis, interpreted the data, and drafted the manuscript. Both authors contributed revisions of the manuscript.

Competing Interests

The authors declare no competing interests.

References

[1] WMO: *Scientific Assessment of Ozone Depletion: 2022, Global Ozone Research and Monitoring Project* (World Meteorological Organization, 2022). Available at: https://csl.noaa.gov/assessments/ozone/2022/downloads/.

[2] Solomon, S., et al. Emergence of healing in the Antarctic ozone layer. *Science* **353**, 269–274 (2016).

[3] Kuttippurath, J., & Nair, P. J. The signs of Antarctic ozone hole recovery. *Scientific Reports*, **7**, 585, (2017).

[4] Petrescu, R. V., Aversa, R., Apicella, A., & Petrescu, F. I. NASA sees first in 2018 the direct proof of ozone hole recovery. *Journal of Aircraft and Spacecraft Technology* **2**, 53–64 (2018).

[5] Stone, K. A., Solomon, S., Kinnison, D. E., & Mills, M. J. On recent large Antarctic ozone holes and ozone recovery metrics. *Geophysical Research Letters* **48** (2021), e2021GL095232.

[6] Weber, M., et al. Global total ozone recovery trends attributed to ozone-depleting substance (ODS) changes derived from five merged ozone datasets. *Atmospheric Chemistry and Physics* **22**, 6843–6859 (2022).

[7] Montzka, S. A., et al. Hydrofluorocarbons (HFC's) Chapter 2 in *Scientific Assessment of Ozone Depletion: 2018, Global Ozone Research and Monitoring Project* – Report No. 58. (World Meteorological Organization, 2018). Available at: https://ozone.unep.org/sites/default/files/2019-05/SAP-2018-Assessment-report.pdf

[8] Rigby, M., et al. Increase in CFC-11 emissions from eastern China based on atmospheric observations. *Nature* **569**, 546–550 (2019).

[9] Benish, S. E., Salawitch, R. J., Ren, X., He, H., & Dickerson, R. R. Airborne observations of CFCs over Hebei province, China in Spring 2016. *Journal of Geophysical Research: Atmospheres*, **126** (2021), e2021JD035152. Wiley Online Library.

[10] Daniel, J. S., Velders, G. J. M., Solomon, S., McFarland, M., & Montzka, S. A. Present and future sources and emissions of halocarbons: Toward new constraints. *Journal of Geophysical Research: Atmospheres*, **112** (2007).

[11] Lickley, M., et al. Quantifying contributions of chlorofluorocarbon banks to emissions and impacts on the ozone layer and climate. *Nature Communications*, **11**, 1380 (2020).

[12] Lickley, M., Fletcher, S., Rigby, M., & Solomon, S. Joint inference of CFC lifetimes and banks suggests previously unidentified emissions. *Nature Communications*, **12**, 2920 (2021).

[13] Lickley, M. J., Daniel, J. S., Fleming, E. L., Reimann, S., & Solomon, S. Bayesian assessment of chlorofluorocarbon (CFC), hydrochlorofluorocarbon (HCFC) and halon banks suggest large reservoirs still present in old equipment. *Atmospheric Chemistry and Physics*, 22(17), 11125–11136 (2022).

[14] United Nations. *Montreal protocol on substances that deplete the ozone layer.* (United Nations, 1987).

[15] Technology and Economic Assessment Panel (TEAP). *Report of the Technology and Economic Assessment Panel Volume 1: Progress Report.* (United Nations Environmental Programme, 2020).

[16] Medical and Chemical Technical Options Committee (MCTOC). *Report of the Medical and Chemical Technical Options Committee: 2022 Assessment.* (United Nations Environmental Programme, 2022).

[17] Technology and Economic Assessment Panel (TEAP), *Report of the Technology and Economic Assessment Panel Volume 1: Progress Report.* (United Nations Environmental Programme, 2023).

[18] Laube, J. C., et al. Newly detected ozone-depleting substances in the atmosphere. *Nature Geoscience*, **7**, 266–269 (2014).

[19] Adcock, K. E., et al. Continued increase of CFC-113a (CCl_3CF_3) mixing ratios in the global atmosphere: emissions, occurrence and potential sources. *Atmospheric Chemistry and Physics*, **18**, 4737–4751 (2018).

[20] Laube, J. C., et al. Tropospheric observations of CFC-114 and CFC-114a with a focus on long-term trends and emissions. *Atmospheric Chemistry and Physics*, 16(23), 15347–15358 (2016).

[21] Vollmer, M. K., et al. Unexpected nascent atmospheric emissions of three ozone-depleting hydrochlorofluorocarbons. *Proceedings of the National Academy of Sciences* **118** (2021), e2010914118.

[22] Western, L. M., et al. Global increase of ozone-depleting chlorofluorocarbons from 2010 to 2020. *Nature Geoscience* **16**, 309–313 (2023).

[23] Daniel, J. S., et al. Scenarios and Information for Policymakers. In *Scientific Assessment of Ozone Depletion*, **278**, 509 (World Meteorological Organization, 2022).

[24] Buendia, C., et al. Refinement to the 2006 IPCC Guidelines for National Greenhouse Gas Inventories Task Force on National Greenhouse Gas Inventories. *Wetlands, IPCC Kyoto* (2019).

[25] Velders, G. J. M., et al. Projections of hydrofluorocarbon (HFC) emissions and the resulting global warming based on recent trends in observed abundances and current policies. *Atmospheric Chemistry and Physics* **22**, 6087–6101 (2022).

[26] A. J. Sicard, & Baker, R. T. Fluorocarbon refrigerants and their syntheses: Past to present. *Chemical Reviews* **120**, 9164–9303 (2020).

[27] Vollmer, M. K., et al. Atmospheric histories and emissions of chlorofluorocarbons CFC-13 ($CClF_3$), ΣCFC-114 ($C_2Cl_2F_4$), and CFC-115 (C_2ClF_5). *Atmospheric Chemistry and Physics* **18**, 979–1002 (2018).

[28] Scott, J. D. & Steven, R. A. Chemical process for the manufacture of 1,1,1,2-tetrafluoroethane. U.S. Patent 5382722A (Jan. 1995).

[29] Piepho, E., Wilmet, V., & Buyle, O. Pentafluoroethane Production Method. U.S. Patent 7067707 (June 2006).

[30] Nose, M., Takahashi, K., & Shibanuma, T. Method for Producing Pentafluoroethane. U.S. Patent 8975455 (2015).

[31] McCulloch, A., & Lindley, A. A. From mine to refrigeration: a life cycle inventory analysis of the production of HFC-134a. *International Journal of Refrigeration*,**26**, 865–872 (2003).

[32] Shanthan Rao, P., Narsaiah, B., Rambabu, Y., Sridhar, M., & Raghavan, K. V. Catalytic processes for fluorochemicals: Sustainable alternatives, in *Industrial Catalysis and Separations: Innovations for Process Intensification*, ed. K. V. Raghavan, B. M. Reddy, 407–435, (Apple Academic Press, Toronto, 2015).

[33] Zhang, S., et al. Life cycle assessment and economic analysis of HFC-134a production from natural gas compared with oil-based and coal-based production. *Frontiers of Chemical Science and Engineering* **16**, 1713–1725 (2022).

[34] Vollmer, M. K., et al. Abrupt reversal in emissions and atmospheric abundance of HCFC-133a (CF_3CH_2Cl). *Geophysical Research Letters* **42**, 8702–8710 (2015).

[35] Chemical Technical Options Committee (CTOC). *Report of the Chemical Technical Options Committee*. (United Nations Environmental Programme, 2014).

[36] Gumprecht, W. H., Longoria, J. M., & Christoph, F. J. Process for manufacture of 1,1-dichlorotetrafluoroethane. European Patent 0426343A1 (1991).

[37] Morikawa, S., Samejima, S., Yositake, M., & Tatematsu, S. Process for Producing 1,1,1,2-Tetrafluoroethane. U.S. 5426253 (1994).

[38] Rigby, M., et al. Re-evaluation of the lifetimes of the major CFCs and CH_3CCl_3 using atmospheric trends. *Atmospheric Chemistry and Physics*, **13**, 2691–2702 (2013).

[39] Technology and Economic Assessment Panel (TEAP). *Report of the Technology and Economic Assessment Panel Volume 1: Progress Report.* (United Nations Environmental Programme, 2021).

[40] Hossaini, R., et al. On the atmospheric budget of ethylene dichloride and its impact on stratospheric chlorine and ozone (2002–2020). *EGUsphere*, 1–29 (2024).

[41] Montzka, S. A., et al. A decline in global CFC-11 emissions during 2018-2019. *Nature*, **590**, 428–432 (2021).

[42] Friedlingstein, P., et al. Global Carbon Budget 2023. *Earth System Science Data*, **15**, 5301–5369 (2023).

[43] Andersen, S. O., et al. Narrowing feedstock exemptions under the Montreal Protocol has multiple environmental benefits. *Proceedings of the National Academy of Sciences*, **118** (2021), e2022668118.

[44] Rust, D., et al. First Atmospheric Measurements and Emission Estimates of HFO-1336mzz(Z). *Environmental Science & Technology* **57**, 11903–11912 (2023).

[45] Ko, M. K., et al. Recommended values for steady-state atmospheric lifetimes and their uncertainties. *SPARC Report on the Lifetimes of Stratospheric Ozone-Depleting Substances, Their Replacements, and Related Species*. 6–1 (2013).

[46] WMO: *Scientific Assessment of Ozone Depletion: 2002, Global Ozone Reasearch and Monitoring Project* — Report No. 47, (World Meteorological Organization, 2003). Available at: https://library.wmo.int/doc_num.php?explnum_id=7306.

[47] Groppelli, G., Fattore, V., Vecchio, M., & Castellan, A. Catalyst Based on Aluminum Fluoride for the Fluorination in Gaseous Phase of Hydrocarbons. U.S. Patent 3787331 (1974).

[48] Poole, D., & Raftery, A. E. Inference for deterministic simulation models: the Bayesian melding approach. *Journal of the American Statistical Association* **95**, 1244–1255 (2000).

[49] Bates, S. C., Cullen, A., & Raftery, A. E. Bayesian uncertainty assessment in multicompartment deterministic simulation models for environmental risk assessment. *Environmetrics: The official journal of the International Environmetrics Society*, **14**(4), 355–371 (2003).

[50] Burkholder, J. B. Appendix A: Summary of Abundances, Lifetimes, ODPs, REs, GWPs, and GTPs. *Scientific Assessment of Ozone Depletion*, **58** (2018).

[51] Davis, M. E., Bernard, F., McGillen, M. R., Fleming, E. L., & Burkholder, J. B. UV and infrared absorption spectra, atmospheric lifetimes, and ozone depletion and global warming potentials for CCl_2FCCl_2F (CFC-112), CCl_3CClF_2 (CFC-112a), CCl_3CF_3 (CFC-113a), and CCl_2FCF_3 (CFC-114a). *Atmospheric Chemistry and Physics*, **16**(12), 8043–8052 (2016).

[52] Prinn, R., et al. The Advanced Global Atmospheric Gases Experiment (AGAGE) Data, *Environmental System Science Data Infrastructure for a Virtual Ecosystem* 2022.

[53] AFEAS: 2001 database. (2001). Retrieved March 10, 2022, from https://agage.mit.edu/data/afeas-data.

[54] Fisher, D. A., & Midgley, P. M. The production and release to the atmosphere of CFCs 113, 114 and 115. *Atmospheric Environment. Part A. General Topics*, **27**, 271–276 (1993).

[55] Climate Change Secretariat, UNFCCC: National Inventory Submissions 2020 to the United Nations Framework Convention of Climate Change. (Bonn, Germany, 2021). Last accessed: May 2024. Available at: http://unfccc.int.

[56] Li, Y.-X., Zhang, Z.-Y., An, M.-D., Gao, D., & Yi, L.-Y. The estimated schedule and mitigation potential for hydrofluorocarbons phase-down in China. *Advances in Climate Change Research*, 10(3), 174–180 (2019).

[57] Say, D., et al. Emissions of halocarbons from India inferred through atmospheric measurements. *Atmospheric Chemistry and Physics* **19**, 9865–9885 (2019).

[58] Prinn, R. G., et al. History of chemically and radiatively important atmospheric gases from the Advanced Global Atmospheric Gases Experiment (AGAGE). *Earth System Science Data* **10**, 985–1018 (2018).

[59] Montzka, S. A., et al. Recent Trends in Global Emissions of Hydrochlorofluorocarbons and Hydrofluorocarbons: Reflecting on the 2007 Adjustments to the Montreal Protocol. *The Journal of Physical Chemistry A*, **119**, 4439-4449 (2015).

[60] Ashford, P., Clodic, D., McCulloch, A., & Kuijpers, L. Emission profiles from the foam and refrigeration sectors comparison with atmospheric concentrations. Part 1: Methodology and data. *International Journal of Refrigeration*, **27**(7), 687–700 (2004).

[61] Cunnold, D. M., et al. Global trends and annual releases of CCl_3F and CCl_2F_2 estimated from ALE/GAGE and other measurements from July 1978 to June 1991. *Journal of Geophysical Research: Atmospheres*, **99**, 1107–1126 (1994).

[62] Hong, B., Strawderman, R. L., Swaney, D. P., & Weinstein, D. A. Bayesian estimation of input parameters of a nitrogen cycle model applied to a forested reference watershed, Hubbard Brook Watershed Six. *Water Resources Research*, **41** (2005).

[63] Rubin, D. B. Using the SIR algorithm to simulate posterior distributions, in: *Bayesian statistics 3. Proceedings of the third Valencia international meeting, 1-5 June 1987*, 395–402 (1988).

[64] Burkholder, J. B., & Hodnebrog, O. Appendix A: Summary of Abundances, Lifetimes, ODPs, REs, GWPs, and GTPs. *Scientific Assessment of Ozone Depletion: 2022, GAW Report No. 278* (2022).

Supplementary Files

This is a list of supplementary files associated with this preprint. Click to download.

- HFCpipelineSINatComs.pdf